



OPEN

SUBJECT AREAS:
MOLECULAR BIOLOGY
CARDIOVASCULAR DISEASES
DRUG DEVELOPMENTReceived
8 August 2014Accepted
17 November 2014Published
4 December 2014Correspondence and
requests for materials
should be addressed to
P.Y. (yupeng_jxndefy@
hotmail.com) or G.H.X.
(xuguohai@sina.com)

Sevoflurane Postconditioning Protects Rat Hearts against Ischemia-Reperfusion Injury via the Activation of PI3K/AKT/mTOR Signaling

Jing Zhang¹, Chen Wang², Shuchun Yu¹, Zhenzhong Luo¹, Yong Chen¹, Qin Liu¹, Fuzhou Hua¹, Guohai Xu¹ & Peng Yu³¹Department of Anesthesiology, the Second Affiliate Hospital of Nanchang University, Nanchang, 330000, China, ²Department of Anesthesiology, the Second Affiliate Hospital of Soochow University, Suzhou, 215000, China, ³Department of Cardiology, the Second Affiliate Hospital of Nanchang University, Nanchang, 330000, China.

Phosphatidylinositol 3-kinase (PI3K)/protein kinase B (AKT) pathway plays a key role in myocardial ischemia-reperfusion (I/R) injury. Mammalian target of rapamycin (mTOR), a downstream target of PI3K/AKT signaling, is necessary and sufficient to protect the heart from I/R injury. Inhaled anesthetic sevoflurane is widely used in cardiac surgeries because its induction and recovery are faster and smoother than other inhaled anesthetics. Sevoflurane proved capable of inducing postconditioning effects in the myocardium. However, the underlying molecular mechanisms for sevoflurane-induced postconditioning (SPC) were largely unclear. In the present study, we demonstrated that SPC protects myocardium from I/R injury with narrowed cardiac infarct focus, increased ATP content, and decreased cardiomyocyte apoptosis, which are mainly due to the activation of PI3K/AKT/mTOR signaling and the protection of mitochondrial energy metabolism. Application of dactolisib (BEZ235), a PI3K/mTOR dual inhibitor, abolishes the up-regulation of pho-AKT, pho-GSK, pho-mTOR, and pho-p70s6k induced by SPC, hence abrogating the anti-apoptotic effect of sevoflurane and reducing SPC-mediated protection of heart from I/R injury. As such, this study proved that PI3K/AKT/mTOR pathway plays an important role in SPC induced cardiac protection against I/R injury.

Coronary artery disease and ischemic heart disease remain a major cause of death and morbidity worldwide. Reperfusion for a rapid recovery of blood and oxygen supply is a standard treatment for myocardial ischemia, whereas transient injury following ischemia, i.e. ischemia-reperfusion (I/R) injury, is also initiated¹. The volatile anesthetic sevoflurane emerged as an important cardioprotective agent in I/R injury of rats, mice², rabbits³, pigs⁴ and in coronary artery disease⁵ of human beings. Sevoflurane produces anesthesia of excellent quality, possesses little systemic toxicity, and undergoes limited biotransformation⁶. Currently, sevoflurane is widely used in cardiac surgeries because the induction and recovery associated with it are faster and smoother than that of other inhaled anesthetics. Despite the forcefully protective effects of sevoflurane preconditioning (SPreC), the clinical application of the treatment has not been used broadly, mainly because this process must be instituted before the ischemic event⁷. In contrast with SPreC, the more promising approach to cardioprotection, “sevoflurane postconditioning” is a protective stimulus administered just before reperfusion and can be easily performed as a post-ischemic intervention to decrease myocardial injury in patients undergoing off-pump coronary artery bypass graft. Therefore, sevoflurane postconditioning (SPC) seems capable of providing effective protection and does not require any previous information of the ischemic event. Previous studies have also found that SPC reduced apoptosis after myocardial I/R injury^{8,9}, essentially protecting the myocardial against I/R injury via various molecular mechanisms, i.e. extracellular regulated protein kinases (ERK), cyclooxygenase-2 (COX-2), signal transducer and activator of transcription 3 (STAT3) and phosphatidylinositol 3-kinase (PI3K)/protein kinase B (AKT) signaling^{10–12}.

The PI3K/AKT/mammalian target of rapamycin (mTOR) pathway plays a key role in normal cellular functions including proliferation, adhesion, migration, invasion, energy metabolism, protein synthesis and pro-survival^{9,13,14}. The PI3K associated signaling pathway is a classical cardioprotective pathway against I/R injury¹⁵ and the



cardioprotective effects of PI3K signaling under SPC are well accepted. mTOR, the downstream of PI3K/AKT signaling, is necessary and sufficient to protect the heart against I/R injury¹⁶. However, it was unknown whether the activation of mTOR is involved in SPC-induced cardioprotection, the potential molecular mechanisms underlying SPC are complex and are not yet well elucidated.

Accordingly, we hypothesize that PI3K/mTOR activation is involved in sevoflurane induced cardioprotective signaling and that this activation inhibits apoptosis. To date, multiple mTOR inhibitors are clinically approved to treat several cancer types and to prevent restenosis after arterial angioplasty¹⁷. Notably, BEZ235 is a novel and potent dual PI3K/mTOR inhibitor in laboratory experiments that is currently being evaluated in clinical trials for advanced solid tumor cancers^{17–19}. Administration of BEZ235 in isolated hearts could reverse the cardioprotective effects of SPC. The data provided in this study showed for the first time that BEZ235 abolished the anti-apoptotic effect of SPC by inhibiting PI3K/mTOR signaling. The mechanisms of SPC exert its cardioprotective effects by the inhibition of PI3K/mTOR associated apoptosis and protection of mitochondrial energy metabolism. Illumination of the involvement of PI3K/AKT/mTOR pathway in sevoflurane-induced cardioprotection may have important clinical implications for the development of cardioprotective strategies.

Results

Sevoflurane postconditioning reduces myocardial infarction size, and improves cardiac function and hemodynamic performance following I/R. To determine the protective effect of SPC on

myocardial I/R, we explored the myocardial infarction size, cardiac function, and hemodynamics. In accordance with a previous study²⁰, our experiment demonstrated that left anterior descending (LAD) coronary ligation induced significant infarction ($50.96 \pm 3.72\%$ of the total area). As shown in Figure 1a, treatment of rat with 1.0 minimum alveolar concentration (MAC) sevoflurane substantially attenuated I/R induced myocardial infarction. The infarct size of SPC group was significantly smaller compared with the I/R group ($21.09 \pm 2.67\%$ vs. $50.96 \pm 3.72\%$, $P < 0.05$). However, the infarction size was no significant difference between SHAM group and SEVO group ($P > 0.05$, Figure 1a).

Consistent with loss of viable myocardium, we observed impaired left ventricular contractility. Cardiac function was examined by echocardiography after I/R. As shown in Figure 1b and Table 1, study on left ventricular systolic function showed there was no statistical significance between SHAM group and SEVO group ($P > 0.05$). However, the systolic function was profoundly decreased in the I/R group, with segmental left ventricular wall dysfunction and resulting decreases in ejection fraction (EF)%, fractional shortening (FS)% and stroke volume (SV, $P < 0.05$). For cardiac remodeling, I/R injury caused significant reductions in interventricular septal thickness at diastolic phase (IVSd), interventricular septal thickness at systolic phase (IVSs), left ventricular posterior wall thickness at diastolic phase (LVPWd), left ventricular posterior wall thickness at systolic phase (LVPWs), as well as dramatic increases in left ventricular internal diameter at diastolic phase (LVIDd) and left ventricular internal diameter at systolic phase (LVIDs, $P < 0.05$). In contrast, SPC administration significantly blunted the reductions of EF%, FS%

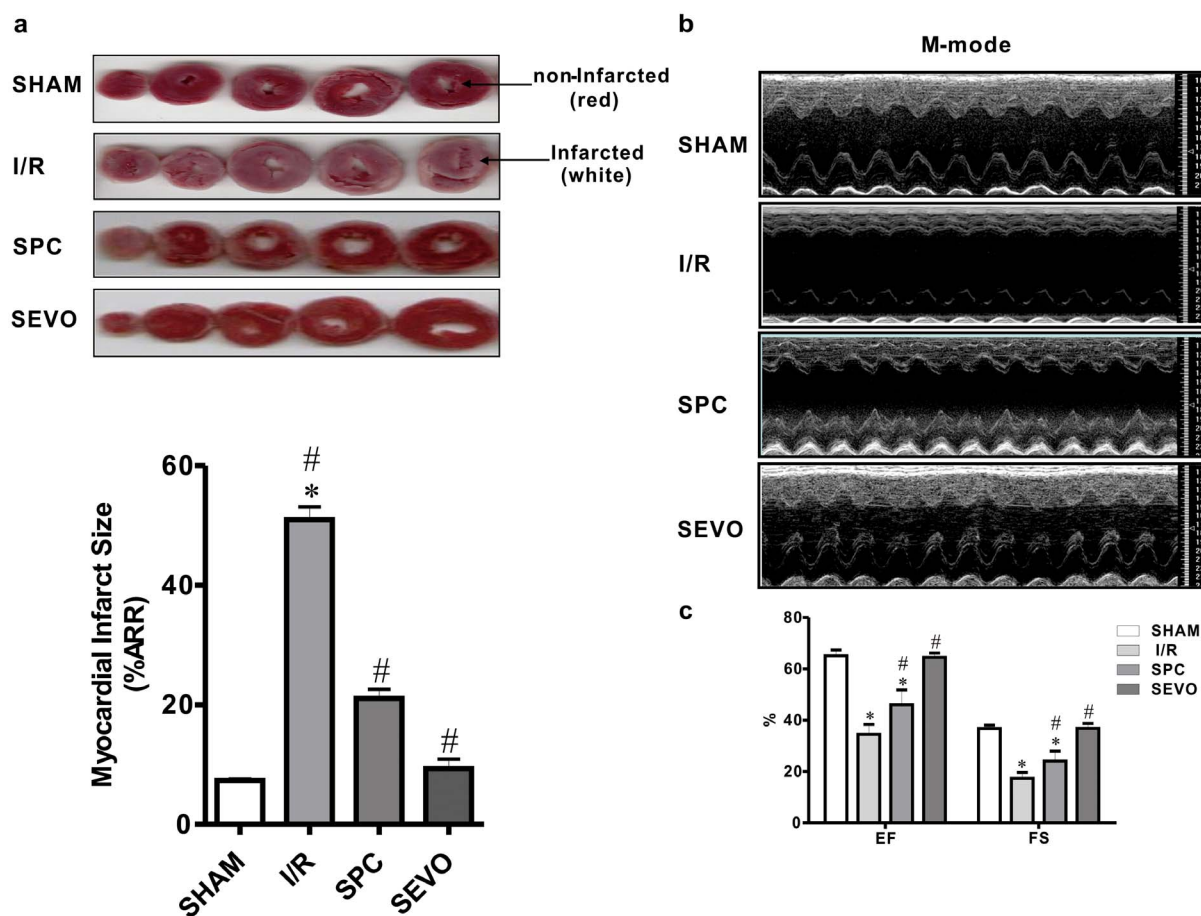


Figure 1 | SPC reduced cardiac infarct size, and improved cardiac function and hemodynamic performance following I/R. (a) Myocardial infarct size. $n = 6$ /group. (b) Representative M-mode images of echocardiography. $n = 10$ /group. (c) EF% and FS% were found to be significantly lower in I/R group as compared with SHAM and SPC group. * $P < 0.05$ compared with SHAM group, # $P < 0.05$ compared with I/R group.



and SV caused by I/R injury ($P < 0.05$ vs. I/R group, Figure 1c). Meanwhile, indicators of cardiac remodeling were improved in the SPC group ($P < 0.05$ vs. I/R group, Table 1).

We also evaluated hemodynamic performance in rats treated with or without SPC. No significant differences in heart rate (HR), mean arterial blood pressure (MAP), and rate pressure product (RPP) at the baseline in all groups ($P > 0.05$, Supplementary Table S1). Decreases in HR, MAP and RPP were observed during reperfusion in all experimental groups ($P < 0.05$ vs baseline). LAD occlusion significantly decreased hemodynamic performance as indicated by reductions in HR, MAP and RPP compared with the SHAM group ($P < 0.05$). SPC significantly increased the hemodynamic parameters compared with the I/R group during reperfusion ($P < 0.05$, Supplementary Table S1). Furthermore, the additional histology data indicated that SPC preserved the integrity of cardiomyocytes well (Supplementary Figure S3).

Collectively, the results demonstrated that SPC decreased cardiac infarct size and improved impaired cardiac function following myocardial I/R injury, and sevoflurane alone did not show any effect on the myocardium without I/R injury.

Sevoflurane postconditioning alleviates myocardial ultrastructural disorder and mitochondrial damage, improves myocardial energy metabolism, and decreases the expression level of p-AMPK. Energy depletion, evidenced by the loss of ATP, damaged mitochondria, and broken energy transfer via creatine-phosphocreatine system, is considered to be a centric factor in the development of cardiac contractile insufficiency^{21,22}. To determine whether SPC improves cardiac contractile insufficiency, we detected myocardial ultrastructure by transmission electron microscopy (TEM) and energy metabolism. TEM images of ultrathin sections showed the ultrastructural changes of the myocardium in the rats in Figure 2a. Cardiomyocytes were clearly observed in well-arranged sarcomeres and intercalated disc manner in the SHAM group, as well as normal mitochondria with no swelling, intact cristae density, and other ultrastructures. However, in some heart sections from the I/R group, I/R resulted in marked ultrastructural damages recognized by absent and edematous separation of sarcomeres. Additionally, vacuolation of the mitochondria with a more pronounced derangement and mitochondrial membrane and cristae disruption were observed in the I/R group. In the SPC group, treatment with sevoflurane showed obvious protection with relatively parallel arrangement of sarcomeres and normal structure of mitochondria. However, mild cytoplasmic rarefaction with mild edema could still be seen. Figure 2a shows the existence of mitochondrial dysfunction after I/R. As the Mitochondria occupy 35–40% of mammalian cardiomyocyte volume and supply 95% of the heart's ATP, the occurrence of mitochondrial dysfunction correlated with ATP levels²³. Thus, we first observed the myocardial ATP content. The ATP content in

the I/R group was significantly less than that in SHAM group (822.79 ± 31.01 vs. 276.29 ± 34.90 $\mu\text{mol/gprot}$, $P < 0.05$, Figure 2b). However, the ATP content of SPC group remained higher than that of the I/R group, but lower than that of the SHAM group ($P < 0.05$).

Furthermore, we examined the transcriptional levels of the genes related to mitochondrial function. As shown in Figure 2c, the mRNA levels of NADH dehydrogenase (ubiquinone) 1 alpha subcomplex subunit 4 (Ndufa4), NADH dehydrogenase (ubiquinone) 1 alpha subcomplex subunit 8 (Ndufa8), cytochrome c oxidase subunit VIIa polypeptide 2 (Cox7a2), and transcription factor A mitochondrial (TFAM) were significantly lower in the I/R and SPC groups as compared to the SHAM group ($P < 0.05$). Further, compared with the I/R group, the mRNA levels of Ndufa4, Ndufa8, Cox7a2 and TFAM were increased by 101.3%, 120.2%, 64.3% and 121.1% in SPC group, respectively ($P < 0.05$). Aside from this observation, the expressions of Ndufa4, Ndufa8, Cox7a2 and TFAM proteins in all experimental groups showed similar trend in the mRNA levels (Figure 2d). Therefore, we concluded that SPC significantly improved the normal transmission of energy and the expression of ATP synthesis associated genes and proteins.

Based on previous findings demonstrating that ATP depletion rapidly induced the activation of the energy sensor adenosine 5' monophosphate-activated protein kinase (AMPK), as well as the importance of AMPK cross-talk with cardiac mitochondria dysfunction²⁴, we asked whether SPC influences the expression of p-AMPK. After 2 h reperfusion, an obvious increase in p-AMPK was demonstrated in the I/R and SPC groups compared with the SHAM group ($P < 0.05$). However, the level of p-AMPK in SPC treated I/R hearts was markedly lower than that in untreated I/R hearts (0.58 ± 0.09 vs. 1.01 ± 0.23 , $P < 0.05$, Figure 2e).

Sevoflurane postconditioning inhibits myocardial apoptosis.

Mitochondrial abnormalities and activation of AMPK could be causes as well as results of apoptosis activation^{24–26}. We examined cardiomyocytes apoptosis in all of the experimental groups. Afterwards, apoptotic cardiomyocytes was detected using terminal deoxynucleotidyl nickend labeling (TUNEL) staining (Figure 3a). Apoptotic index of the cardiomyocytes was significantly lower in the SPC group when compared with the I/R group ($77.8 \pm 5.12\%$ vs. $132 \pm 9.20\%$, $P < 0.05$, Figure 3b).

To further investigate the effect of SPC on the expression of apoptosis related proteins, the levels of pro-apoptotic proteins cleaved Caspase-3 and Bax and anti-apoptotic protein Bcl2 in cardiac left ventricular were detected by western blot. Compared with the sham control, Figure 3c shows that I/R injury significantly up-regulated the cleaved Caspase-3 level and Bax/Bcl2 ratio in both I/R and SPC groups ($P < 0.05$). However, the cleaved Caspase-3 level was higher by 49.7% in the I/R group than in the SPC group. Furthermore, the

Table 1 | Cardiac function measured by echocardiography

Cardiac function	SHAM (n = 10)	I/R (n = 10)	SPC (n = 10)	SEVO (n = 6)
EF (%)	65.10 ± 2.29	34.53 ± 3.82*	46.02 ± 5.50**	64.51 ± 1.42#
FS (%)	36.78 ± 1.35	17.38 ± 2.26*	24.10 ± 3.66**	36.16 ± 1.65#
SV (ml)	172.89 ± 23.68	106.31 ± 14.60*	131.94 ± 10.16**	171.35 ± 28.83#
LVIDd (mm)	6.79 ± 0.65	7.76 ± 0.77*	6.78 ± 0.38#	6.77 ± 0.55#
LVIDs (mm)	4.38 ± 0.46	6.38 ± 0.55*	5.17 ± 0.19**	4.27 ± 0.27#
IVSd (mm)	1.53 ± 0.23	1.08 ± 0.20*	1.43 ± 0.25#	1.49 ± 0.09#
IVSs (mm)	2.21 ± 0.42	1.45 ± 0.37*	1.72 ± 0.42**	2.10 ± 0.27#
LVPWd (mm)	1.62 ± 0.21	1.36 ± 0.47	1.40 ± 0.30#	1.56 ± 0.08
LVPWs (mm)	2.08 ± 0.24	1.44 ± 0.30*	1.62 ± 0.45**	2.01 ± 0.19#

* $P < 0.05$ vs SHAM group;

** $P < 0.05$ vs I/R group. # vs age and weight matched rat. EF: ejection fraction; FS: fractional shortening; SV: stroke volume; LVIDd: left ventricular internal diameter at diastolic phase; LVIDs: left ventricular internal diameter at systolic phase; IVSd: interventricular septal thickness at diastolic phase; IVSs: interventricular septal thickness at systolic phase; LVPWd: left ventricular posterior wall thickness at diastolic phase; LVPWs: left ventricular posterior wall thickness at systolic phase. n = 6 ~ 10/group.

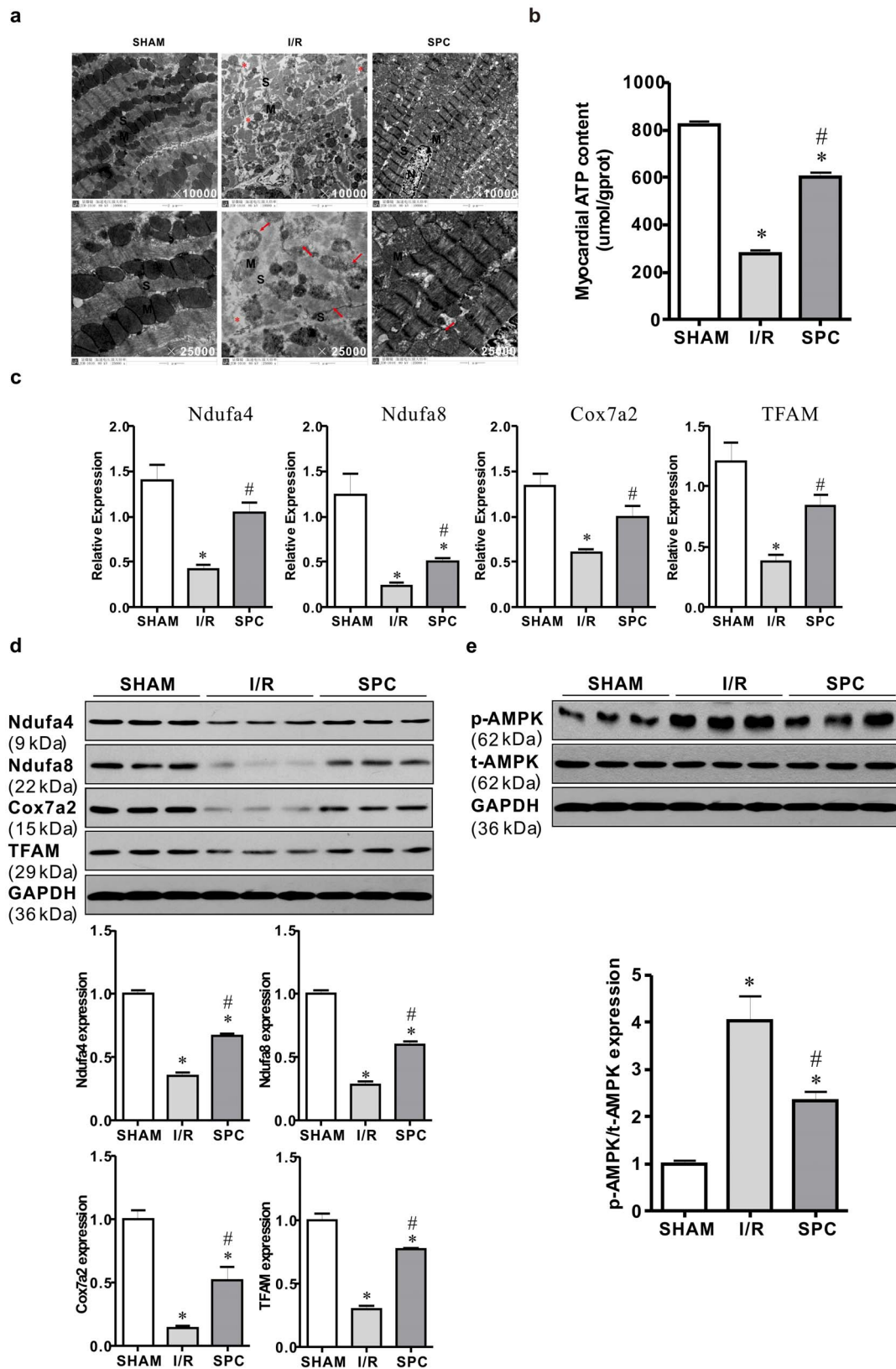


Figure 2 | SPC alleviated myocardial ultrastructural disorder and mitochondrial damage, improved myocardial energy metabolism, and decreased the expression levels of *pho*-AMPK. (a) Representative Transmission electron micrographs at a magnification of 10000 and 25000. Note that myofilaments were absent (*) and sevoflurane postconditioning decreased damaged mitochondria (→). $n = 3/\text{group}$. (b) SPC improved myocardial ATP content in I/R rat hearts. $n = 6/\text{group}$. (c) Real-time PCR was performed for the analysis of the mRNA levels of Ndufa 4, Ndufa 8, Cox7a2 and TFAM. $n = 4/\text{group}$. (d) The immunoblotting for Ndufa 4, Ndufa 8, Cox7a2 and TFAM proteins was performed. $n = 3/\text{group}$. (e) The immunoblotting for p-AMPK and t-AMPK proteins was performed. $n = 3/\text{group}$. * $P < 0.05$ compared with SHAM group, # $P < 0.05$ compared with I/R group. Note that cropped gel images are used in this figure and the gels were run under the same experimental conditions.

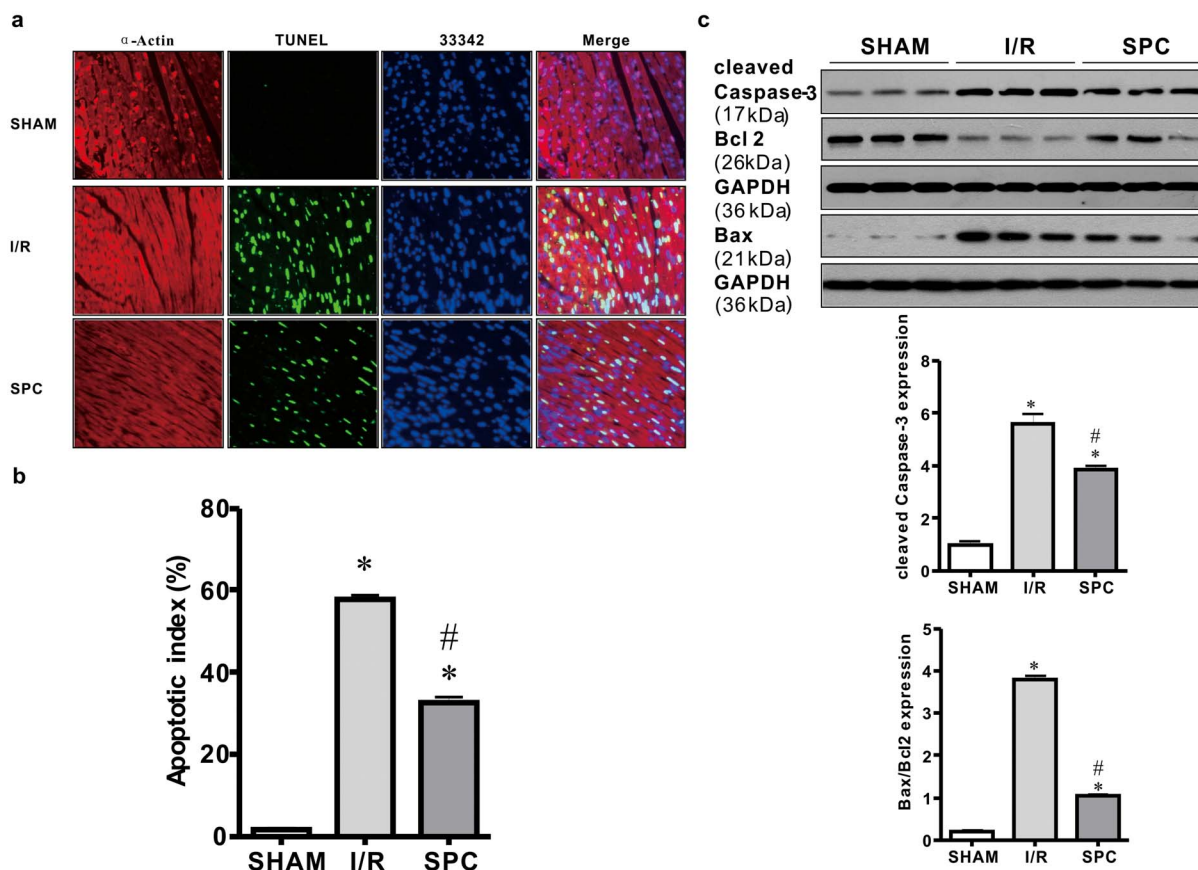


Figure 3 | SPC inhibited myocardial apoptosis *in vivo* rats. (a) Representative photomicrographs of detection of apoptotic cardiomyocytes by TUNEL staining. Red fluorescence shows α -Actin. Green fluorescence shows TUNEL-positive nuclei; Blue fluorescence shows nuclei of total cardiomyocytes. $n = 4/\text{group}$. (b) Apoptotic cardiomyocytes were quantified by apoptotic index which was termed as the percentage of apoptotic cardiomyocytes. $n = 4/\text{group}$. (c) Representative immunoblotting for cleaved Caspase-3, Bcl 2 and Bax was performed. $n = 3/\text{group}$. * $P < 0.05$ compared with SHAM group, # $P < 0.05$ compared with I/R group. Note that cropped gel images are used in this figure and the gels were run under the same experimental conditions.

Bax/Bcl2 ratio was significantly higher in I/R group than that in both SHAM and SPC groups ($P < 0.05$).

Taken together, the data suggest that SPC decreased the activation of cardiomyocytes apoptosis after myocardial I/R injury and that anti-apoptotic effects may be a causative factor for SPC-mediated cardioprotection.

Sevoflurane postconditioning increases the levels of p-AKT, p-GSK, p-mTOR and p-p70s6k in the myocardium following I/R. Activation of the prosurvival PI3K/AKT/mTOR pathway has been shown to be important for cardioprotection in several I/R models^{27,28}. Activation of PI3K/AKT/mTOR pathway, demonstrated as increases in the levels of phosphorylation of AKT, glycogen synthase kinase (GSK), mTOR, and P70 S6 kinase (p70s6k), has been reported to protect against cell apoptosis^{29,30}. We therefore set out to study the effect of SPC on the activation of PI3K/AKT/mTOR signaling in the myocardium following I/R. First, we examined the effect of SPC on AKT and GSK phosphorylation. As shown in Figure 4a, SPC significantly increased the levels of p-AKT/t-AKT and p-GSK/t-GSK in the myocardium compared with I/R group. Next, we examined the level of p-mTOR, which is an important downstream of AKT in hearts. After 2 h of reperfusion following 30 min of ischemia, the levels of p-mTOR/t-mTOR in the hearts were significantly higher in the SPC group than those in the I/R group (1.01 ± 0.10 vs. 0.38 ± 0.11 , $P < 0.05$, Figure 4b). In addition, SPC significantly increased the level of p-p70s6k/t-p70s6k in the myocardium (0.94 ± 0.06) compared with I/R group (0.40 ± 0.03).

Thus, we observed that I/R and SPC significantly increased phosphorylation of AKT/mTOR and its downstream targets GSK and p70s6k after 2 h of reperfusion. However, this increase was much more pronounced in the SPC group ($P < 0.05$). The data suggest that SPC activated the PI3K/AKT/mTOR pathway during myocardial I/R.

Pharmacological inhibition of PI3K/mTOR abrogates SPC-induced cardioprotection against I/R injury in isolated hearts. The above results show that cardioprotection triggered by SPC may be associated with PI3K/AKT/mTOR pathway. To further confirm the direct link between PI3K/AKT/mTOR pathway and SPC mediated cardioprotection, we conducted an isolated experiment. BEZ235, an imidazo [4, 5-c] quinoline derivative and widely used as the inhibitor of PI3K/mTOR signaling, was administered to rats^{17,18}. This optimal dose of BEZ235 was selected from a series of dose-ranging studies, which indicated that cardiac infarct size in 20 $\mu\text{mol/L}$ of BEZ235-treated heart was comparable with the isolated I/R group (Supplementary Figure S4a and Figure 5). As shown in Supplementary Figure S4b, SPC-induced phosphorylation of AKT and mTOR was completely abolished with the treatment of BEZ235 (20 $\mu\text{mol/L}$). Consistent with the *in vivo* results, cardiac infarct size was obviously increased after myocardial I/R injury ($48.78 \pm 3.37\%$), and myocardial infarct size in the SPC group was lower than that of the I/R group ($27.49 \pm 1.31\%$, $P < 0.05$). As is shown in Figure 5, the infarct size was significantly greater in BEZ + SPC group compared with the SPC

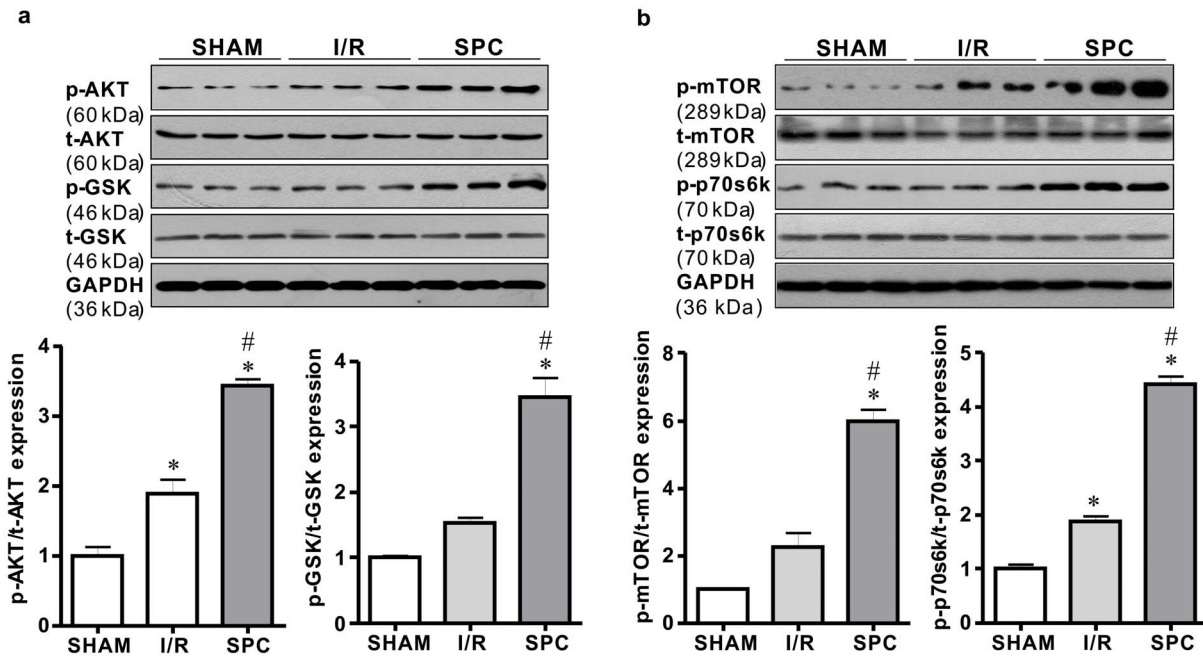


Figure 4 | SPC increased the levels of pho-AKT, pho-GSK, pho-mTOR and pho-p70s6k in the myocardium following I/R. (a) Expressions of p-AKT, t-AKT, p-GSK and t-GSK in hearts were analyzed. $n = 3/\text{group}$. (b) The expressions of p-mTOR, t-mTOR, p-p70s6k and t-p70s6k were analyzed. $n = 3/\text{group}$. * $P < 0.05$ compared with SHAM group, # $P < 0.05$ compared with I/R group. Note that cropped gel images are used in this figure and the gels were run under the same experimental conditions.

group that did not receive the inhibitor ($57.07 \pm 8.39\%$ vs. $27.49 \pm 1.31\%$, $P < 0.05$).

Next, the hemodynamics of all the experimental groups was detected. No differences in baseline hemodynamics were observed among the experimental groups ($P > 0.05$, Supplementary Table S2). At T_1 , T_2 , T_3 and T_4 , the other groups, with the exception of the SHAM group, had significant decreases in HR, left ventricular systolic pressure (LVSP), and $\pm dp/dt_{\max}$, as well as an increase in left ventricular end-diastolic pressure (LVEDP, $P < 0.05$). As expected, SPC significantly inhibited the increases of HR, LVSP and $\pm dp/dt_{\max}$, and restored the reduction of LVEDP relative to I/R group ($P < 0.05$). The BEZ + SPC group treated with BEZ235 did not differ compared with the I/R group ($P > 0.05$).

Combined with *in vivo* experiment, these data suggest that SPC could significantly improve cardiac contractile and diastolic functions and limit myocardial infarction after myocardial I/R injury, and pharmacological inhibition of PI3K/mTOR with BEZ235 abrogated the SPC induced myocardial protection against I/R injury in isolated rat hearts.

Administration of BEZ235 decreases the activation of PI3K/AKT/mTOR pathway in isolated hearts. We examined the effect of BEZ235 treatment on PI3K/AKT/mTOR signaling phosphorylation. The expression of PI3K/AKT/mTOR pathway measured by western blot provided the evidence in support of this notion. As shown in Figures 6a and b, there was no difference in total AKT, GSK,

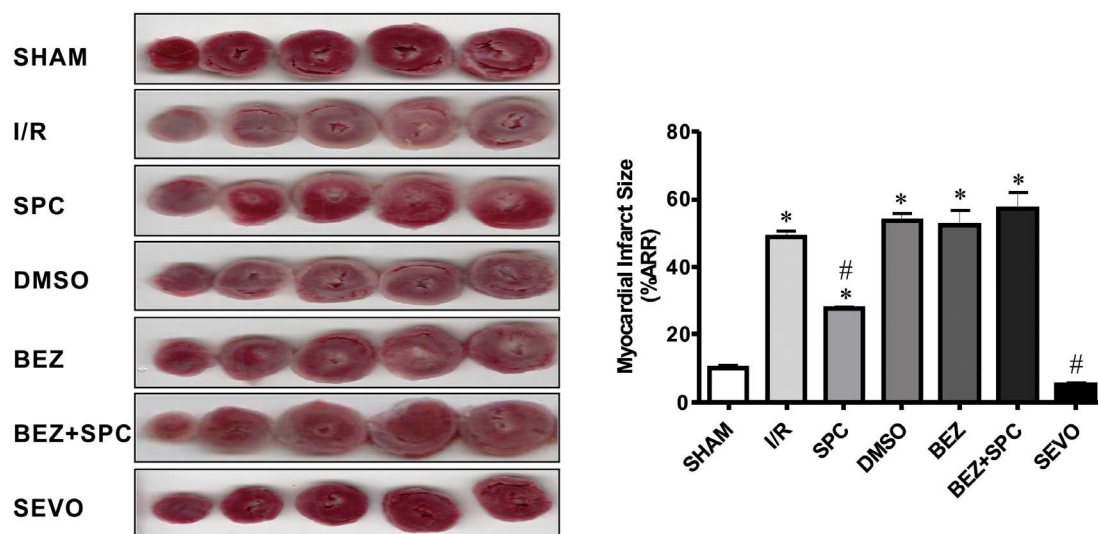


Figure 5 | BEZ235 eliminated SPC-mediated decrease in cardiac infarction. Infarct size was determined using 1% triphenyltetrazolium chloride (TTC) staining. Infarct size was expressed as percent of infarct divided by the total area at risk. $n = 6/\text{group}$. * $P < 0.05$ compared with SHAM group, # $P < 0.05$ compared with I/R group.



mTOR, and p70s6k expressions in different conditions. Consistent with *in vivo* results, SPC significantly increased phosphorylation of AKT, GSK, mTOR and p70s6k ($P < 0.05$ vs I/R group). However, blocking PI3K/mTOR activity with BEZ235 significantly decreased SPC-induced AKT/GSK phosphorylation ($P < 0.05$, Figure 6a). Furthermore, BEZ235 abolished the effects of SPC on p-mTOR and p-p70s6k expressions ($P < 0.05$, Figure 6b). The BEZ235 effectively inhibited the activation of PI3K/AKT/mTOR pathway.

Collectively, based on direct measurement of PI3K associated protein phosphorylation levels, our results indicate that the PI3K pathway is primarily involved in SPC mediated protection in I/R hearts.

Treatment with BEZ235 abolishes the anti-apoptotic effect of SPC in isolated hearts. Consistently, we measured the expressions of pro-apoptotic proteins cleaved Caspase-3 and Bax and anti-apoptotic protein Bcl2 in the all-experimental groups after 2 h reperfusion. Similar to the data *in vivo*, the expressions of cleaved Caspase-3 and Bax/Bcl2 ratio were also increased after I/R injury ($P < 0.05$ vs SHAM group, Figure 7). SPC could significantly induce the down-regulation of the cleaved Caspase-3 and Bax/Bcl2 ratio relative to I/R group ($P < 0.05$). Administration of BEZ235 alone before reperfusion had no effect on I/R induced cardiomyocytes apoptosis. However, BEZ235 could abrogate the SPC induced down-regulation of the cleaved Caspase-3 ($P < 0.05$). In addition, as shown in Figure 7, the ratio of Bax/Bcl2 in BEZ + SPC group was increased by 333.4% compared to the SPC group ($P < 0.05$).

In summary, overall results imply that SPC could decrease myocardial apoptosis after I/R injury and PI3K/AKT/mTOR pathway played a role in the SPC-induced anti-apoptotic effect on cardiomyocytes.

Discussion

I/R injury is a major obstacle to the treatment of acute myocardial infarction; therefore, suppressing myocardial I/R injury still represents a great challenge. Both preconditioning and the newly discovered postconditioning may have a protective effect on I/R injury. Before the occurrence of a severe ischemic episode, the treatment of preconditioning can be beneficial. Unfortunately, the index ischemic episode is often unpredictable in the clinic. Postconditioning is applied after a prolonged period of ischemia and can also alleviate cardiac I/R injury to an extent comparable with that induced by preconditioning. Thus, postconditioning may be more useful in clinical practice.

In the present study, 2.4% sevoflurane was administered for 15 min at the onset of reperfusion following ischemia in myocardial I/R model³¹. We found that SPC significantly improved functional recovery, and the nearly 50% decrease in infarct size after I/R seems consistent with previous studies^{27,28}. The novel finding of this study is that SPC increases the phosphorylation of PI3K/AKT/mTOR pathway *in vivo* and isolated rat models of I/R. Administration of BEZ235 during SPC period blunted PI3K/AKT/mTOR pathway activation and abolished cardioprotection. Our study demonstrated a direct link between PI3K/AKT/mTOR pathway activation and the attenuation of myocardial apoptosis in SPC induced cardioprotection.

SPC is an effective method to reduce I/R injury. It is well accepted that SPC plays a critical role in limiting myocardial infarction, reducing myocardial damage and dysfunction, attenuating ventricular arrhythmias, decreasing cardiomyocytes apoptosis, and preventing heart failure. Furthermore, a recent study demonstrated that SPC has a cytoprotective effect on cell death and inflammation in an *in vitro* model of endotoxaemia using lipopolysaccharide-exposed human endothelial cells³². Therefore, these studies support the idea that SPC serves as a cardiovascular protective strategy.

In vivo, we observed that SPC improved left ventricular systolic dysfunction. Due to blockage of the blood flow in the myocardium,

myocardial I/R leads to an imbalance of energy metabolism and triggers a rapid increase in intracellular calcium, which in turn induces the release of pro-apoptotic factors and reactive oxygen species that are key elements in systolic dysfunction³³. Therefore, improvement of cardiac contractile function was closely associated with the preservation of mitochondrial function³⁴. The result, in effect, proved that SPC attenuated mitochondrial dysfunction induced by I/R injury. Functional integrity of the cardiomyocytes requires an abundance of mitochondria capable of producing ATP; as such, mitochondrial abnormalities were correlated with ATP levels²⁴. Additionally, SPC inhibited the decrease in the mRNA levels of the genes related to mitochondrial function, such as Ndufa4, Ndufa8, Cox7a2 and TFAM. Consistently, we observed significant increases in the translational levels of these genes. We also demonstrated that myocardial ATP content was increased with administration of 1.0 MAC sevoflurane at the onset of reperfusion. Moreover, when cells face metabolic stress, i.e. I/R injury and glucose deprivation, ATP depletion will rapidly activate AMPK, which constitutes a molecular hub for cellular metabolic control³⁵. The role of AMPK during myocardial I/R injury is still controversial. The previous study reported that SPC-induced AMPK activation protects the isolated perfused heart against I/R injury³⁶. However, a recent study demonstrated that SPreC-mediated cardioprotection is partially dependent on the activation of AMPK. In cardiomyocyte specific AMPK α 2 dominant negative transgenic mice, SPreC could also ameliorate cardiac I/R injury *in vivo*³⁷, suggesting that the independence of AMPK on SPreC-generated cardioprotective effect. In our study, we observed that SPC could decrease the expression of p-AMPK protein compared with the I/R group. At least two main possibilities may illustrate this discrepancy, including (i) the previous study showed that the important role of AMPK *in vitro* experiment, an isolated perfused heart in which myocardial energy production is completely glucose dependent. The role of AMPK (a critical regulator of cardiac energy metabolism and cardiomyocyte function) in an isolated perfused heart system differs from the *in vivo* model, (ii) due to the different operating time of SPreC and SPC, the function of AMPK in the different process may also be inconsonant. The present study clearly shows that SPC increased cellular ATP level, decreased the activation of AMPK, protected cardiac cells from energy deprivation.

Alessia Perino et al. reported compelling data that myocardial p110 γ connects cAMP signaling pathways and PtdIns(3,4,5)P3 (the lipid product of PI3K)³⁸. AMPK was negatively regulated by the cAMP/PKA pathway. PI3Ks and their downstream signal transduction enzymes, the downstream target of AMPK, were involved in many critical cellular functions, including protein synthesis, inflammatory responses and apoptosis³⁹. Activation of PI3K recruits cellular protein kinases that in turn activate downstream kinases, including the phosphorylation of AKT and GSK-3 β ⁴⁰. Moreover, phosphorylation of AKT permitted activation of mTOR and p70s6k⁴¹. A large number of studies have shown that the activation of PI3K/AKT/mTOR signaling pathways protect against myocardial I/R injury^{42,43}. However, the relative importance of these kinases mediating the protection in myocardial I/R injury remains disputable. A recent study highlighted that ischemic postconditioning mediated cardioprotection through ERK1/2 but not PI3K/AKT signaling⁴⁴. Park et al. have suggested that pharmacological postconditioning with bradykinin confers cardioprotection at reperfusion by inhibiting the mPTP opening presumably through inactivation of GSK-3 β ⁴⁵. In addition, Schwartz and Lagranha have reported that the activation of PI3K/AKT pathway failed to protect against lethal I/R injury in pigs⁴⁶. In the present study, we observed that PI3K/AKT pathway is activated and that its downstream targets GSK, mTOR, and p70s6k are extremely phosphorylated by SPC. This phosphorylation is commensurate with SPC mediated cardioprotection. More

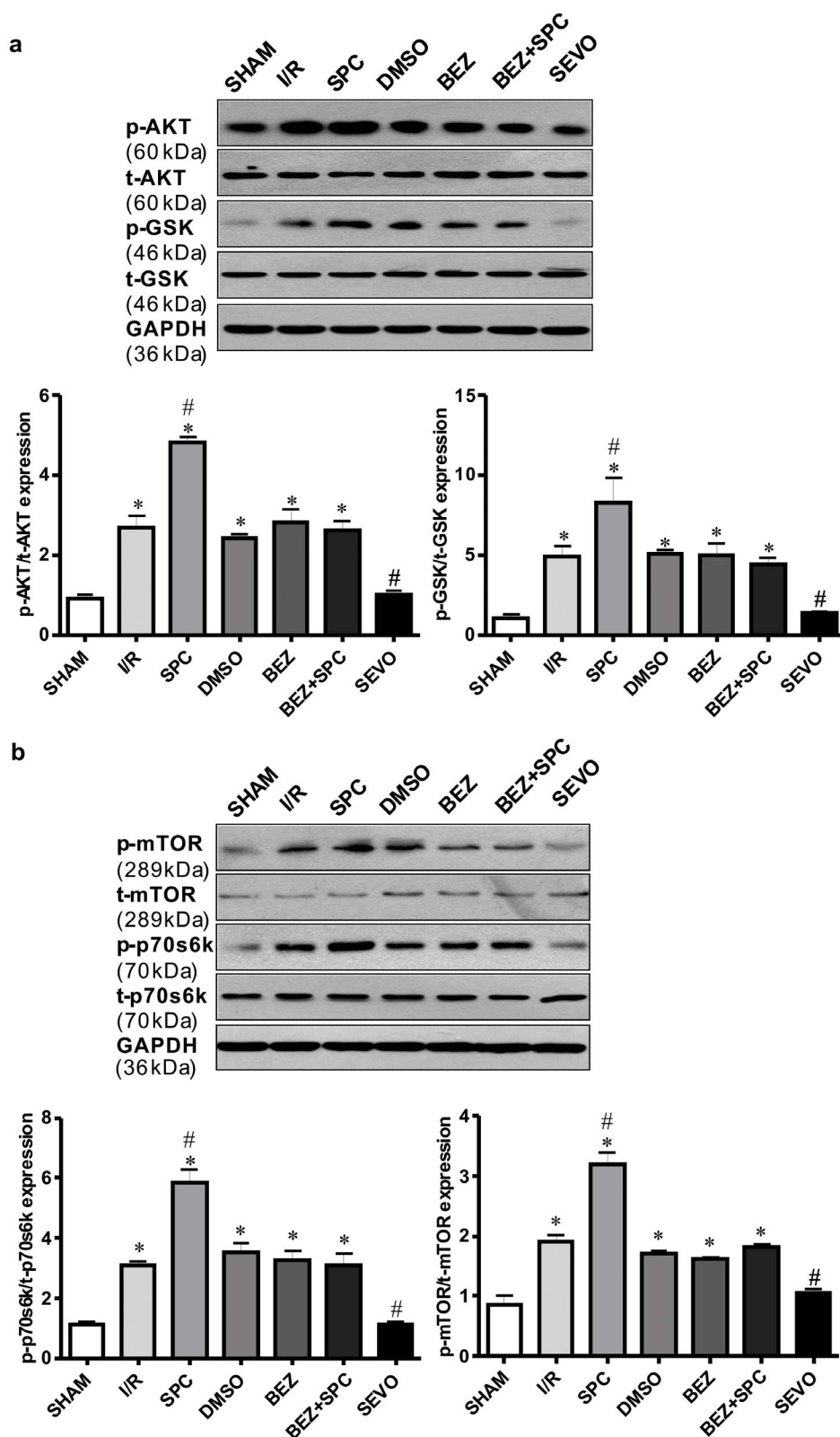


Figure 6 | BEZ235 abolished SPC-mediated activation in PI3K/AKT/mTOR signaling. (a) The panel shows representative p-AKT/t-AKT and p-GSK/t-GSK of the seven experimental groups. $n = 3/\text{group}$. (b) The panel shows representative p-mTOR and p-p70s6k. The p-mTOR and p-p70s6k were normalized against total mTOR and p70s6k expression. $n = 3/\text{group}$. * $P < 0.05$ compared with SHAM group, # $P < 0.05$ compared with I/R group. Note that cropped gel images are used in this figure and the gels were run under the same experimental conditions.

extensive *in vitro* and *in vivo* studies are required to elucidate the unequivocal role of PI3K/AKT/mTOR signaling pathways in the pharmacological postconditioning.

Apoptosis, a form of programmed cell death, is an important mechanism for myocardial I/R injury and the induction of apoptosis was dependent on the suppression of PI3K/AKT/mTOR pathway¹⁷.

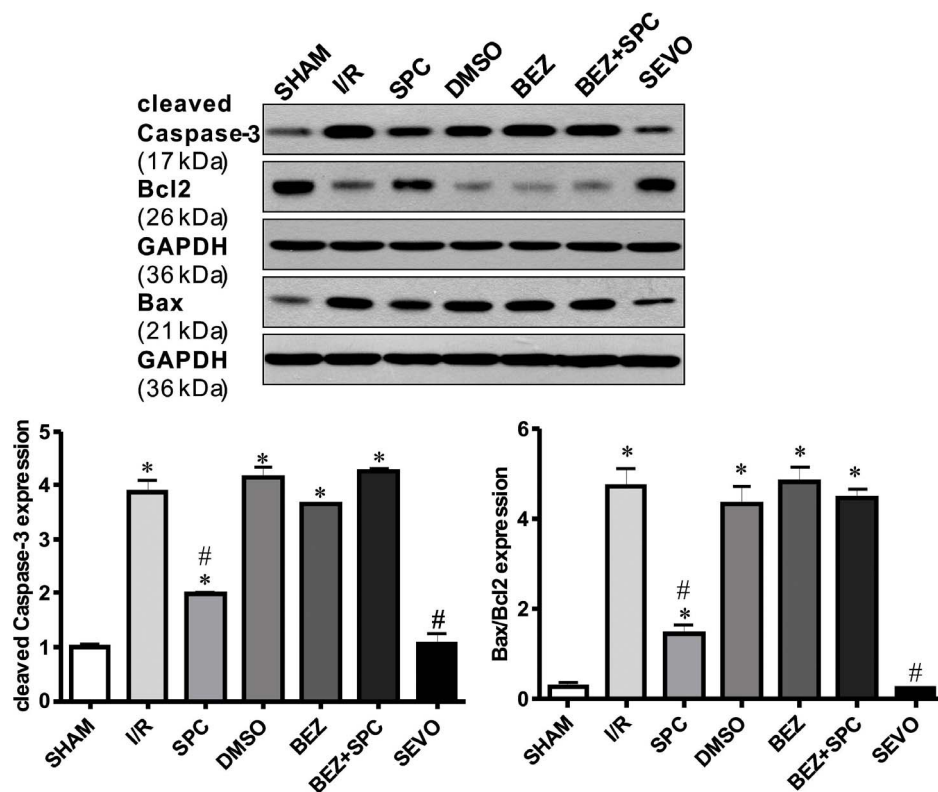


Figure 7 | BEZ235 abrogated the anti-apoptotic effect of sevoflurane postconditioning in isolated hearts. Representative immunoblotting of cleaved Caspase-3, Bcl 2 and Bax from left ventricular samples acquired at the end of reperfusion in the seven groups. The blots for GAPDH were served as loading controls. $n = 3/\text{group}$. * $P < 0.05$ compared with SHAM group, # $P < 0.05$ compared with I/R group. Note that cropped gel images are used in this figure and the gels were run under the same experimental conditions.

Previous studies have shown that SPC protected myocardium against I/R injury via attenuating cardiomyocytes apoptosis¹¹. Our study verified that SPC reduced apoptotic cardiomyocytes, which was marked with the TUNEL staining. The western blot results suggested that SPC activated the PI3K/AKT/mTOR pathway and its downstream Bcl-2, which in turn suppressed the pro-apoptotic activity of apoptosis⁴⁸. We also found that SPC diminished cardiomyocytes apoptosis through down-regulating the levels of pro-apoptotic protein cleaved Caspase-3 and Bax. Therefore, it is possible that anti-apoptotic effect of the PI3K/AKT/mTOR pathway in SPC-treated rat may be responsible for the cardioprotection against I/R injury. To evaluate this hypothesis, we administered BEZ235 in isolated hearts to further investigate the direct relationship between PI3K/AKT/mTOR pathway and the SPC that induced the myocardial protection effect. BEZ235 is an imidazo [4, 5-c] quinoline derivative and widely used as the specific inhibitor of PI3K/mTOR signaling^{17,18}. Administering BEZ235, the PI3K/mTOR dual inhibitor, we initially determined an optimal dose by examining myocardial infarct size in SPC group rat after 15 min reperfusion with BEZ235 at 0, 10, 20 and 50 $\mu\text{mol/L}$, respectively. We noticed that 20 $\mu\text{mol/L}$ was sufficient to completely abolish the SPC induced cardioprotection and the phosphorylation levels of AKT and mTOR. In the study, we found that administration of BEZ235 abrogated the up-regulation of p-AKT, p-GSK, p-mTOR, p-p70s6k and the down-regulation of the cleaved Caspase-3 and Bax/Bcl2 ratio induced by SPC, in effect inhibited the SPC-induced cardioprotection effects. Thus, PI3K/AKT/mTOR pathway has been taken into consideration as one of the most attractive targets for the development of SPC induced cardioprotection. Our results were in agreement with previous reports that activation of this pathway has a remarkably cardioprotective effect on I/R injury. Nevertheless, these results cannot rule out the possibility of some cross-talk between AMPK and apoptosis. In order to obtain a more

comprehensive understanding of this important aspect, more intensive investigations will be done in the near future.

Our findings provide evidence that SPC administration induced cardioprotection *in vivo* and in isolated hearts. SPC-induced cardioprotection was modulated by the activation of PI3K/AKT/mTOR pathway, protection of mitochondria, and anti-apoptotic effect on cardiomyocytes. These data are significant because they demonstrate that the PI3K/AKT/mTOR pathway is not only a key regulator of normal cellular functions, but also a pivotal player in the mediation of cardioprotection.

Methods

Animals. Adult, healthy male Sprague-Dawley rats, weighing 180–230 g and of healthy grade were approved by the Committee of the Medical College of Soochow University (Suzhou, People's Republic of China; License Number: 20020008 Grade II). All animals were maintained at the Model Animal Research Center of Soochow University. All experiments were performed in accordance with the guidelines for the Principles of Laboratory Animal Care and Use of Laboratory Animals published by NIH (NIH Publication, 8th Edition, 2011). The Soochow University Committee on Animal Care approved all aspects of our animal care methodology and experimental protocol.

Myocardial I/R injury *in vivo* surgical preparation. Rats were anaesthetized with sodium pentobarbital (50 mg/kg) and heparinized (1000 IU/kg) by intraperitoneal injection to ensure that pedal and palpebral reflexes were absent throughout the experimental protocol⁴⁹. Rats were acutely instrumented for the measurement of systemic hemodynamics as previously described⁵⁰. Rats were briefly and mechanically ventilated with room air to maintain arterial pH, PCO_2 and PO_2 within the normal physiological range. A thoracotomy was performed in the left fifth intercostal space, and the pericardium was opened. A 6-0 silk suture was placed around the proximal LAD appendage for 2–3 mm through a small polytetra fluoroethylene tube, which formed a snare. LAD occlusion was produced by pulling the snare for 30 min and confirmed by epicardial cyanosis, while successful reperfusion was achieved by loosening the snare for 2 h and verified by epicardial hyperemic. A polyethylene catheter placed into the left ventricle and connecting a pressure transducer to a data acquisition system (Medlab-U/4C501H system) was used to measure hemodynamic data. Hemodynamic parameters, including HR, MAP, and RPP, were recorded at



30 min of equilibration (T_0), 30 min (T_1), 60 min (T_2), 90 min (T_3), and 2 h (T_4) after reperfusion.

Langendorff isolated heart model preparation. Rats were anaesthetized by intraperitoneal injection of sodium pentobarbital (50 mg/kg) and heparinized (1000 IU/kg). Once surgical anesthesia was achieved (confirmed by no response to tail clamping), the hearts were quickly excised after median sternotomy and mounted on a modified non-circulating Langendorff apparatus via aorta cannulation for retrograde perfusion at constant pressure (80 mmHg) with Krebs-Henseleit (K-H) buffer (pH 7.40 ± 0.05 , $37.0 \pm 0.5^\circ\text{C}$). The buffer was continuously gassed with 95% $\text{O}_2 + 5\% \text{CO}_2$ ⁵¹. Langendorff apparatus was assembled as described previously⁵². K-H solution configuration (mmol/L): NaCl 118.0, KCl 4.8, KH_2PO_4 1.2, NaHCO_3 25.0, MgSO_4 1.2, CaCl_2 2.5, glucose 11.0. A small latex balloon connected to a cuff pressure transducer (SIA Industrial & Trade, Beijing, China) was inserted into the left ventricle through the mitral valve to monitor the heart function. The balloon was filled with bubble-free saline to set a stable LVEDP at 10 mmHg, and the balloon volume remained unchanged during the following experiment. The indicators were determined LVSP, LVEDP, $\pm dp/dt_{\text{max}}$ and HR by Med Lab 6.0 software. Rats with refractory ventricular fibrillation, frequent arrhythmia, LVSP < 75 mmHg or HR < 180 beats/min were excluded.

Myocardial infarction size measurement. Myocardial infarction size was determined by 2,3,5-triphenyltetrazolium chloride triazole (TTC; T8877, Sigma-Aldrich Co., St. Louis, MO, USA) staining. At the end of 2 h reperfusion, the rat hearts were removed rapidly and frozen at -20°C for 2 h, then cut into 5 pieces in cross-section. The hearts were incubated in 1% TTC in 0.1 mol/L phosphate buffer solution (pH 7.4) at 37°C for 10 min, and subsequently fixed overnight in 10% formalin. Then, myocardial infarct area (white color) could be differentiated from the area at risk (red color). The infarct size was calculated for each slice, and reported as the percent of infarct divided by the total area at risk by Alpha Ease FC Imaging System. For myocardial infarct size determination, six hearts ($n = 6/\text{group}$) were assessed in each experimental group.

Echocardiography evaluation. Two-dimensional echocardiography measurements were conducted after 2 h of reperfusion. Cardiac function was studied by M-mode echocardiography using the Vevo770 system equipped with a 35-MHz linear transducer as previous methods⁵³. Rats were anaesthetized with sodium pentobarbital (50 mg/kg, intraperitoneal). The adequacy of anesthesia was assayed by the disappearance of righting reflex and pedal withdrawal reflex. The measurement was operated by an independent professional ultrasound technician. Parameters of cardiac function were obtained in the M-mode tracings and averaged using ≥ 5 cardiac cycles ($n = 10/\text{group}$).

Myocardial ATP content measurement. Myocardial ATP concentration was determined by using a bioluminescence method⁵⁴. A luminometric method based on the luciferin-luciferase reaction was used to quantify ATP in myocardium by using an ATP assay kit (A095, Jiancheng Bioengineering Institute, Nanjing, China). The concentration of phosphocreatine in myocardium was determined by using the reverse phase-high performance liquid chromatography. The concentration of glycogen in myocardium was determined with a chemistry colorimetry method by using a glycogen detection kit (A043, Jiancheng Bioengineering Institute, Nanjing, China). For myocardial ATP content measurement, six hearts ($n = 6/\text{group}$) were assessed in each experimental group.

Transmission electron microscopy. Rat hearts were rapidly removed at the end of reperfusion for detecting myocardial ultrastructural alterations by TEM. Briefly, a small piece (1 mm³) of tissue was dissected from left ventricular and cut into ultrathin sections (50–80 nm) while fixed with an ultramicrotome. Longitudinal sections were collected on 200 mesh copper grids and stained with 1% uranylacetate, and visualized on an H-600 electron microscope (Hitachi Limited, Tokyo, Japan). Sections were examined with TEM by an independent investigator. Three fields ($n = 3/\text{group}$) were examined for each sample at 10000 and 25000 magnification.

Analysis of mRNAs by real time-PCR. According to the instruction of the manufacturer, total RNA was extracted from cardiac tissues using trizol reagent (15596-018, Invitrogen, Carlsbad, California, USA) as described⁵⁵. Total RNA (2 μg) was subjected for first strand complementary DNA (cDNA) synthesis by using the oligo (dT) first strand primer. After cDNA synthesis, the expression levels of Ndufa4, Ndufa8, Cox7a2, TFAM were evaluated by real time-PCR using the FastStart Universal SYBR Green Master (4913850001, Roche, Indianapolis, USA). The β -actin was used as an internal control and the primers used in the experiments were shown in Supplementary Table S3 ($n = 4/\text{group}$).

Western blot analysis. Cardiac left ventricular samples were collected at the end of reperfusion and cellular protein extracts were prepared. Briefly, the samples were homogenized using a RIPA lysis buffer (20–188, Millipore, Billerica, MA, USA) and a complete mammalian proteinase inhibitor cocktail (PI101, Roche Diagnostics GmbH, Mannheim, Germany). Homogenates were centrifuged at 12000 g for 20 min at 4°C to isolate total protein. The clarified supernatant was used to quantify protein. Protein concentrations were determined using a bicinchoninic acid protein assay kit (23227, Thermo, MA, USA). After been denatured, equivalent amount of proteins (30 μg) were separated by 12% SDS-polyacrylamide gel electrophoresis and then

transferred onto a polyvinylidene fluoride (PVDF) membrane. After blocking with 5% non-fat milk for 1 h, the PVDF membranes were appropriately incubated with the following primary antibodies: p-AMPK α 1/2 (1 : 1000; BS5003, Bioworld, Minneapolis, MN), t-AMPK α 1/2 (1 : 1000; BS5003, Bioworld, Minneapolis, MN), p-AKT (1 : 1000; 4058, Cell Signaling Technology, Colorado, USA), t-AKT (1 : 1000; 4685, Cell Signaling Technology, Colorado, USA), p-GSK (1 : 1000; 9323, Cell Signaling Technology, Colorado, USA), t-GSK (1 : 1000; 9315, Cell Signaling Technology, Colorado, USA), p-mTOR (1 : 1000; 5536, Cell Signaling Technology, Colorado, USA), t-mTOR (1 : 1000; 2983, Cell Signaling Technology, Colorado, USA), p-p70s6k (1 : 1000; 9234, Cell Signaling Technology, Colorado, USA), t-p70s6k (1 : 1000; 2708, Cell Signaling Technology, Colorado, USA), Ndufa4 (1 : 500; BS3883, Bioworld, Minneapolis, MN), Ndufa8 (1 : 500; BS3336, Bioworld, Minneapolis, MN), Cox7a2 (1 : 500; BS60288, Bioworld, Minneapolis, MN), TFAM (1 : 1000; sc-166965, Santa Cruz, California, USA), cleaved Caspase-3 (1 : 1000; sc-22171-R, Santa Cruz, California, USA), Bax (1 : 1000; sc-526, Santa Cruz, California, USA), and Bcl-2 (1 : 1000; sc-492, Santa Cruz, California, USA) at 4°C overnight, followed by incubation with peroxidase conjugated secondary antibodies. The signals were visualized with the enhanced pierce chemiluminescence (Pierce, Rockford, IL, USA). To control for lane loading, the same membranes were probed with anti-GAPDH (1 : 1000; AG019, Beyotime Institute of Biotechnology, Shanghai, China). Quantitative analysis of the signals was performed by scanning densitometry and the results from each experimental group were expressed as relative integrated intensity compared with that of sham control hearts ($n = 3/\text{group}$).

Cardiomyocyte apoptosis analysis. Cardiac tissues at papillary muscle level were collected for paraffin sectioning. Paraffin sections were stained with the TUNEL assay kit (G3250, Promega, Madison, WI, USA) to examine cardiomyocyte apoptosis according to the instruction of the manufacturer. The images of cardiomyocyte apoptosis in the sections were captured with a fluorescent microscope (Zeiss Ltd., Germany). For the measurement of TUNEL activity, all images were randomly examined under identical conditions. Four hearts ($n = 4/\text{group}$) were detected in each experimental group.

Statistical analysis. The results are shown as means \pm standard deviation ($\bar{x} \pm sd$). Comparisons between the groups were analyzed by using one-way analysis of variance (ANOVA) followed by Tukey multiple comparison post test (Tukey's test), $P < 0.05$ was considered to be statistical significance.

- Zhang, Y. & Ren, J. Targeting autophagy for the therapeutic application of histone deacetylase inhibitors in ischemia/reperfusion heart injury. *Circulation* **129**, 1088–1091 (2014).
- Li, H. *et al.* Isoflurane postconditioning reduces ischemia-induced nuclear factor-kappaB activation and interleukin 1beta production to provide neuroprotection in rats and mice. *Neurobiol Dis* **54**, 216–224 (2013).
- Lange, M. *et al.* Desflurane-induced postconditioning is mediated by beta-adrenergic signaling: role of beta 1- and beta 2-adrenergic receptors, protein kinase A, and calcium/calmodulin-dependent protein kinase II. *Anesthesiology* **110**, 516–528 (2009).
- Larsen, J. R., Sivesgaard, K., Christensen, S. D., Honge, J. L. & Hasenkam, J. M. Heart rate limitation and cardiac unloading in sevoflurane post-conditioning. *Acta Anaesthesiol Scand* **56**, 57–65 (2012).
- Orriach, J. L. *et al.* Sevoflurane in intraoperative and postoperative cardiac surgery patients. Our experience in intensive care unit with sevoflurane sedation. *Curr Pharm Des* **19**, 3996–4002 (2013).
- Holaday, D. A. & Smith, F. R. Clinical characteristics and biotransformation of sevoflurane in healthy human volunteers. *Anesthesiology* **54**, 100–106 (1981).
- Kloner, R. A. & Rezkalla, S. H. Preconditioning, postconditioning and their application to clinical cardiology. *Cardiovasc Res* **70**, 297–307 (2006).
- Inamura, Y., Miyamae, M., Sugioka, S., Domae, N. & Kotani, J. Sevoflurane postconditioning prevents activation of caspase 3 and 9 through antiapoptotic signaling after myocardial ischemia-reperfusion. *J Anesth* **24**, 215–224 (2010).
- Bader, A. G., Kang, S., Zhao, L. & Vogt, P. K. Oncogenic PI3K deregulates transcription and translation. *Nat Rev Cancer* **5**, 921–929 (2005).
- Chen, H. T. *et al.* Cardioprotection of sevoflurane postconditioning by activating extracellular signal-regulated kinase 1/2 in isolated rat hearts. *Acta Pharmacol Sin* **29**, 931–941 (2008).
- Drenger, B. *et al.* Diabetes blockade of sevoflurane postconditioning is not restored by insulin in the rat heart: phosphorylated signal transducer and activator of transcription 3- and phosphatidylinositol 3-kinase-mediated inhibition. *Anesthesiology* **114**, 1364–1372 (2011).
- Stumpner, J. *et al.* The Role of Cyclooxygenase-1 and -2 in Sevoflurane-Induced Postconditioning Against Myocardial Infarction. *Semin Cardiothorac Vasc Anesth* **18**, 272–280 (2014).
- Engelman, J. A., Luo, J. & Cantley, L. C. The evolution of phosphatidylinositol 3-kinases as regulators of growth and metabolism. *Nat Rev Genet* **7**, 606–619 (2006).
- Fry, M. J. Structure, regulation and function of phosphoinositide 3-kinases. *Biochim Biophys Acta* **1226**, 237–268 (1994).
- Cuadrado, I., Fernandez-Velasco, M., Bosca, L. & de Las Heras, B. Labdane diterpenes protect against anoxia/reperfusion injury in cardiomyocytes: involvement of AKT activation. *Cell Death Dis* **2**, e229 (2011).



16. Aoyagi, T. *et al.* Cardiac mTOR protects the heart against ischemia-reperfusion injury. *Am J Physiol Heart Circ Physiol* **303**, H75–85 (2012).
17. Santulli, G. & Totary-Jain, H. Tailoring mTOR-based therapy: molecular evidence and clinical challenges. *Pharmacogenomics* **14**, 1517–1526 (2013).
18. Wilson, T. R. *et al.* Widespread potential for growth-factor-driven resistance to anticancer kinase inhibitors. *Nature* **487**, 505–509 (2012).
19. Fallahi-Sichani, M., Honarnejad, S., Heiser, L. M., Gray, J. W. & Sorger, P. K. Metrics other than potency reveal systematic variation in responses to cancer drugs. *Nat Chem Biol* **9**, 708–714 (2013).
20. Luedde, M. *et al.* RIP3, a kinase promoting necroptotic cell death, mediates adverse remodelling after myocardial infarction. *Cardiovasc Res* **103**, 206–216 (2014).
21. Neubauer, S. The failing heart—an engine out of fuel. *N Engl J Med* **356**, 1140–1151 (2007).
22. Neubauer, S. *et al.* Myocardial phosphocreatine-to-ATP ratio is a predictor of mortality in patients with dilated cardiomyopathy. *Circulation* **96**, 2190–2196 (1997).
23. Pham, T., Loisel, D., Power, A. & Hickey, A. J. Mitochondrial inefficiencies and anoxic ATP hydrolysis capacities in diabetic rat heart. *Am J Physiol Cell Physiol* **307**, C499–507 (2014).
24. Green, D. R. & Reed, J. C. Mitochondria and apoptosis. *Science* **281**, 1309–1312 (1998).
25. Nieminen, A. I. *et al.* Myc-induced AMPK-phospho p53 pathway activates Bak to sensitize mitochondrial apoptosis. *Proc Natl Acad Sci U S A* **110**, E1839–1848 (2013).
26. Liang, J. *et al.* The energy sensing LKB1-AMPK pathway regulates p27(kip1) phosphorylation mediating the decision to enter autophagy or apoptosis. *Nat Cell Biol* **9**, 218–224 (2007).
27. Zhu, M. *et al.* Ischemic postconditioning protects remodeled myocardium via the PI3K-PKB/Akt reperfusion injury salvage kinase pathway. *Cardiovasc Res* **72**, 152–162 (2006).
28. Rahman, S. *et al.* Phosphorylation of GSK-3 β mediates intralipid-induced cardioprotection against ischemia/reperfusion injury. *Anesthesiology* **115**, 242–253 (2011).
29. Li, L. *et al.* Ribonuclease inhibitor up-regulation inhibits the growth and induces apoptosis in murine melanoma cells through repression of angiogenin and ILK/PI3K/AKT signaling pathway. *Biochimie* **103**, 89–100 (2014).
30. Janku, F., Kaseb, A. O., Tsimberidou, A. M., Wolff, R. A. & Kurzrock, R. Identification of novel therapeutic targets in the PI3K/AKT/mTOR pathway in hepatocellular carcinoma using targeted next generation sequencing. *Oncotarget* **5**, 3012–3022 (2014).
31. Obal, D. *et al.* One MAC of sevoflurane provides protection against reperfusion injury in the rat heart in vivo. *Br J Anaesth* **87**, 905–911 (2001).
32. Rodríguez-González, R. *et al.* Effects of sevoflurane postconditioning on cell death, inflammation and TLR expression in human endothelial cells exposed to LPS. *J Transl Med* **11**, 87 (2013).
33. Carreira, R. S., Lee, P. & Gottlieb, R. A. Mitochondrial therapeutics for cardioprotection. *Curr Pharm Des* **17**, 2017–2035 (2011).
34. Doenst, T., Nguyen, T. D. & Abel, E. D. Cardiac metabolism in heart failure: implications beyond ATP production. *Circ Res* **113**, 709–724 (2013).
35. Inoki, K., Zhu, T. & Guan, K. L. TSC2 mediates cellular energy response to control cell growth and survival. *Cell* **115**, 577–590 (2003).
36. Lamberts, R. R. *et al.* Reactive oxygen species-induced stimulation of 5'AMP-activated protein kinase mediates sevoflurane-induced cardioprotection. *Circulation* **120**, S10–15 (2009).
37. Zhao, J. *et al.* Sevoflurane preconditioning attenuates myocardial ischemia/reperfusion injury via caveolin-3-dependent cyclooxygenase-2 inhibition. *Circulation* **128**, S121–129 (2013).
38. Perino, A. *et al.* Integrating Cardiac PIP 3 and cAMP Signaling through a PKA Anchoring Function of p110 γ . *Mol Cell* **42**, 84–95 (2011).
39. Gioran, A., Nicotera, P. & Bano, D. Impaired mitochondrial respiration promotes dendritic branching via the AMPK signaling pathway. *Cell Death Dis* **5**, e1175 (2014).
40. Fumarola, C., Bonelli, M. A., Petronini, P. G. & Alfieri, R. R. Targeting PI3K/AKT/mTOR pathway in non small cell lung cancer. *Biochem Pharmacol* **90**, 197–207 (2014).
41. Tasian, S. K., Teachey, D. T. & Rheingold, S. R. Targeting the PI3K/mTOR Pathway in Pediatric Hematologic Malignancies. *Front Oncol* **4**, 108 (2014).
42. Zhang, L., Wang, H., Xu, J., Zhu, J. & Ding, K. Inhibition of cathepsin S induces autophagy and apoptosis in human glioblastoma cell lines through ROS-mediated PI3K/AKT/mTOR/p70S6K and JNK signaling pathways. *Toxicol Lett* **228**, 248–259 (2014).
43. Cantley, L. C. The phosphoinositide 3-kinase pathway. *Science* **296**, 1655–1657 (2002).
44. Darling, C. E. *et al.* Postconditioning via stuttering reperfusion limits myocardial infarct size in rabbit hearts: role of ERK1/2. *Am J Physiol Heart Circ Physiol* **289**, H1618–1626 (2005).
45. Park, S. S., Zhao, H., Mueller, R. A. & Xu, Z. Bradykinin prevents reperfusion injury by targeting mitochondrial permeability transition pore through glycogen synthase kinase 3 β . *J Mol Cell Cardiol* **40**, 708–716 (2006).
46. Schwartz, L. M. & Lagranha, C. J. Ischemic postconditioning during reperfusion activates Akt and ERK without protecting against lethal myocardial ischemia-reperfusion injury in pigs. *Am J Physiol Heart Circ Physiol* **290**, H1011–1018 (2006).
47. Maiese, K., Chong, Z. Z., Shang, Y. C. & Wang, S. Targeting disease through novel pathways of apoptosis and autophagy. *Expert Opin Ther Targets* **16**, 1203–1214 (2012).
48. Zinkel, S., Gross, A. & Yang, E. BCL2 family in DNA damage and cell cycle control. *Cell Death Differ* **13**, 1351–1359 (2006).
49. Wang, C. *et al.* Extracellular signal-regulated kinases trigger isoflurane preconditioning concomitant with upregulation of hypoxia-inducible factor-1 α and vascular endothelial growth factor expression in rats. *Anesth Analg* **103**, 281–288 (2006).
50. Qiao, S. *et al.* Delayed anesthetic preconditioning protects against myocardial infarction via activation of nuclear factor- κ B and upregulation of autophagy. *J Anesth* **27**, 251–260 (2013).
51. Varadarajan, S. G., An, J., Novalija, E. & Stowe, D. F. Sevoflurane before or after ischemia improves contractile and metabolic function while reducing myoplasmic Ca(2+) loading in intact hearts. *Anesthesiology* **96**, 125–133 (2002).
52. Liao, R., Podesser, B. K. & Lim, C. C. The continuing evolution of the Langendorff and ejecting murine heart: new advances in cardiac phenotyping. *Am J Physiol Heart Circ Physiol* **303**, H156–167 (2012).
53. Zhang, X. *et al.* Involvement of reductive stress in the cardiomyopathy in transgenic mice with cardiac-specific overexpression of heat shock protein 27. *Hypertension* **55**, 1412–1417 (2010).
54. Kordas, K. S. *et al.* ATP and ATPase secretion by exocrine pancreas in rat, guinea pig, and human. *Pancreas* **29**, 53–60 (2004).
55. Wang, D., Malo, D. & Hekimi, S. Elevated mitochondrial reactive oxygen species generation affects the immune response via hypoxia-inducible factor-1 α in long-lived Mcl1 +/- mouse mutants. *J Immunol* **184**, 582–590 (2010).

Acknowledgments

This study was supported by the National Natural Science Foundation of China (Grant No. H1501) and the Technology Bureau Research Fund of Suzhou, China (Grant No. SYS2012085). We are grateful to Dr Zhixiang Xu (University of Alabama at Birmingham) for carefully reading and revising the manuscript.

Author contributions

P.Y., G.X. and C.W. designed the study. J.Z., P.Y., S.Y., Z.L. and Y.C. performed all experiments. P.Y. and J.Z. also performed the data analysis and drafted the manuscript. Q.L. and F.H. participated in data analysis. G.X. and C.W. critically revised the manuscript. All authors reviewed the final manuscript.

Additional information

Supplementary information accompanies this paper at <http://www.nature.com/scientificreports>

Competing financial interests: The authors declare no competing financial interests.

How to cite this article: Zhang, J. *et al.* Sevoflurane Postconditioning Protects Rat Hearts against Ischemia-Reperfusion Injury via the Activation of PI3K/AKT/mTOR Signaling. *Sci. Rep.* **4**, 7317; DOI:10.1038/srep07317 (2014).



This work is licensed under a Creative Commons Attribution-NonCommercial-NoDerivs 4.0 International License. The images or other third party material in this article are included in the article's Creative Commons license, unless indicated otherwise in the credit line; if the material is not included under the Creative Commons license, users will need to obtain permission from the license holder in order to reproduce the material. To view a copy of this license, visit <http://creativecommons.org/licenses/by-nc-nd/4.0/>